ACS Photonics

pubs.acs.org/journal/apchd5

Article

Exploring the Limit of Multiplexed Near-Field Optical Trapping

Donato Conteduca, Giuseppe Brunetti, Giampaolo Pitruzzello, Francesco Tragni, Kishan Dholakia, Thomas F. Krauss, and Caterina Ciminelli*

Cite This: *ACS Photonics* 2021, 8, 2060–2066

Read Online

ACCESS | Metrics & More | Article Recommendations | Supporting Information

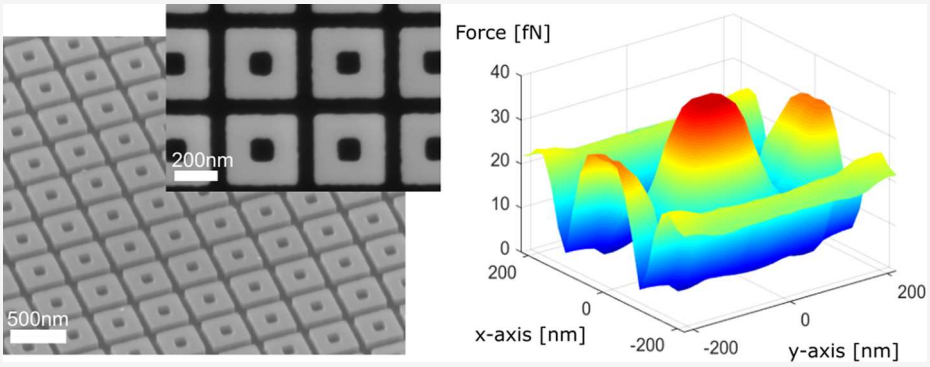

ABSTRACT: Optical trapping has revolutionized our understanding of biology by manipulating cells and single molecules using optical forces. Moving to the near-field creates intense field gradients to trap very smaller particles, such as DNA fragments, viruses, and vesicles. The next frontier for such optical nanotweezers in biomedical applications is to trap multiple particles and to study their heterogeneity. To this end, we have studied dielectric metasurfaces that allow the parallel trapping of multiple particles. We have explored the requirements for such metasurfaces and introduce a structure that allows the trapping of a large number of nanoscale particles (>1000) with a very low total power $P < 26$ mW. We experimentally demonstrate the near-field enhancement provided by the metasurface and simulate its trapping performance. We have optimized the metasurface for the trapping of 100 nm diameter particles, which will open up opportunities for new biological studies on viruses and extracellular vesicles, such as studying heterogeneity, or to massively parallelize analyses for drug discovery.

KEYWORDS: *optical nanotweezers, multiple trapping, dielectric metasurface, near-field trapping, nanophotonics, anapole modes*

The ability to trap and manipulate biological matter by optical forces in a contact-free manner has yielded major advances in the biomedical sciences and has provided new insights into single molecule biophysics and cellular behavior.[1,2] Recently, these capabilities have been extended from the micro- to the nanoscale by the exploitation of near-field effects in photonic nanostructures,[3] where the increased gradient has enabled the trapping of nanoscale objects such as proteins and DNA fragments.[4,5] The main focus of the field thus far has been on the trapping of individual or very few particles.[4,6] On the other hand, biological studies typically require a large number of samples in order to provide meaningful statistics,[7,8] which can be time-consuming and contrasts with the necessity of fast tests and diagnoses in the biomedical field.[9] For this reason, and to capture the inherent heterogeneity of biological samples, researchers have now turned their attention to the possibility of trapping many particles in parallel by multiplexing optical traps in larger arrays.[10,11] This is particularly exciting at the nanoscale because it opens opportunities for novel biological studies.

Nanophotonics offers an efficient solution for nanoscale trapping because of the strong near-field energy localization it provides leading to enhanced gradient forces.[12,13] Nanophotonic structures, both plasmonic and dielectric, can efficiently confine light in localized hotspots that offer a much stronger gradient force for the same input power as equivalent Gaussian beams in conventional free-space optical tweezers.[14,15]

Accordingly, a number of array configurations have now been introduced as nanotweezers for multiplexed trapping.[16,17] For example, photonic nanojets have been used to trap multiple 190 nm size polystyrene nanoparticles, as well as *Escherichia coli* bacteria in parallel.[10] Alternatively, plasmonic

Received: March 8, 2021
Published: July 6, 2021

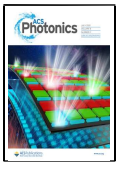

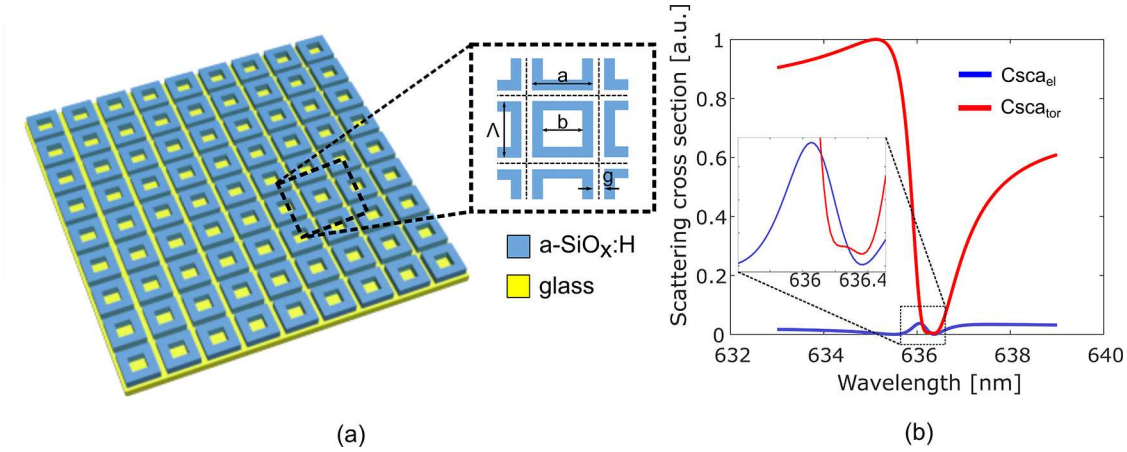

Figure 1. (a) Configuration of the dielectric metasurface based on an array of nanocuboids. (b) Scattering cross sections of the electric (blue curve) dipole ($Csca_{el}$) and toroidal (red curve) dipole ($Csca_{tor}$) with the anapole condition in the inset (dotted line), given by the intersection of both curves, corresponding to the resonance condition of the metasurface. The period for each unit cell is Λ = 430 nm with a total area of an 60 × 60 aray of 665 μm^2.

resonant metasurfaces have been used to demonstrate multiplexed trapping of 20 nm polystyrene nanobeads.[16]

Given these exciting developments, it is necessary to define the scalability of such arrays and to determine the optical power requirement for exciting multiple traps simultaneously. Regarding scalability, we note that lithographically made structures are clearly superior, in particular for large array sizes, with 100′s or 1000′s trapping sites. Regarding power, the enhancement of optical forces given by near-field hotspots and resonant effects should be exploited.[18,19] These arguments clearly favor metasurface-type realizations, either plasmonic or dielectric. While plasmonic structures offer tighter confinement than dielectric ones, their intrinsic Ohmic losses pose significant limitations: (a) lower *Q*-factors, hence, lower resonant enhancement, and (b) lower resonance amplitude, which corresponds to less energy confined in the trapping site on resonance; (c) significant thermal heating, which can lead to convection currents and stronger particles diffusion that destabilize the trapping site.[13,20]

Here, we consider a dielectric metasurface that meets the requirements of scalability and low power operation for a new form of multisite array; our design supports anapole modes with an experimentally demonstrated high *Q*-factor and a significant amplitude enhancement on resonance. The strong amplitude is sometimes overlooked as a parameter, but it is essential for a high energy confinement at the trapping site which is required to achieve stable trapping.[18] In particular, we design the structure for the trapping of 100 nm beads with a refractive index of n = 1.45, which mimics the trapping of single viruses.[21] We numerically demonstrate that for an array of 60 × 60 elements, such a metasurface only requires a power of 39 $\mu W/\mu m^2$, corresponding to a power of about 7 μW for each unit cell and an overall power $P \approx 26$ mW for the trapping of individual objects in each array element, and therefore for the trapping in total of >1000 objects, which is necessary for more exhaustive biological studies.[22,23] For example, in biomedicine, collecting data form a few thousand individual objects is required for achieving statistical relevance, for example, in drug-screening and diagnostics.[24,25]

DESIGN AND EXPERIMENTAL RESULTS

Design and Numerical Results of the Dielectric Metasurface. The dielectric metasurface consists of an array of dielectric nanocuboids in amorphous silicon. The amorphous silicon is deposited onto a glass substrate (n = 1.45) by sputter deposition in a hydrogen/oxygen environment, which causes partial oxidation, thereby extending the operation toward shorter wavelengths and allowing operation, here, at λ = 650 nm (a-SiO_x:H, n = 2.4, $k \sim 5 \times 10^{-4}$ at λ = 650 nm).[26] It is well recognized that operating at a shorter wavelength is advantageous for trapping because the trap stiffness scales as $1/\lambda^4$, with a consequent force enhancement with decreasing wavelength.[27]

The nanocuboid design was chosen following the design of ref 28, whereby the anapole state is obtained via the destructive interference between the electrical and the toroidal radiation modes supported by the array (Figure 1b).[29] Several configurations have been proposed to excite such anapole modes, for example, nanodisks and nanoparticles,[29] but the nanocuboid geometry stands out because of its strong near field confinement and high *Q*-factor in an array configuration.

The nanocuboid metasurface supports the two modes shown in Figure 2a. The first mode at λ = 636 nm is the anapole mode of interest while the second mode at λ = 648 nm does not offer

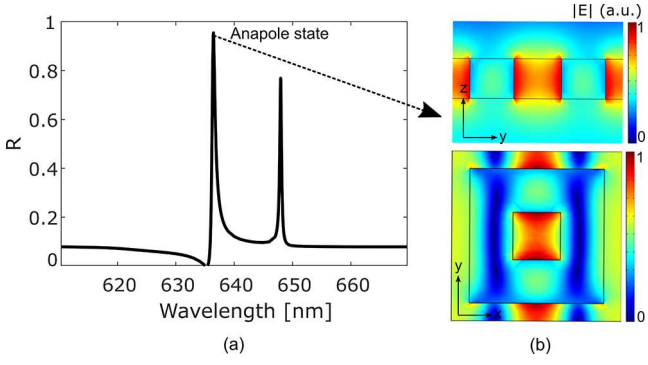

Figure 2. (a) Reflection spectrum of the array of nanocuboids with the anapole state at λ = 636 nm. (b) Cross-section (top) and top view (bottom) of the mode distribution at resonance.

https://doi.org/10.1021/acsphotonics.1c00354
ACS Photonics 2021, 8, 2060−2066

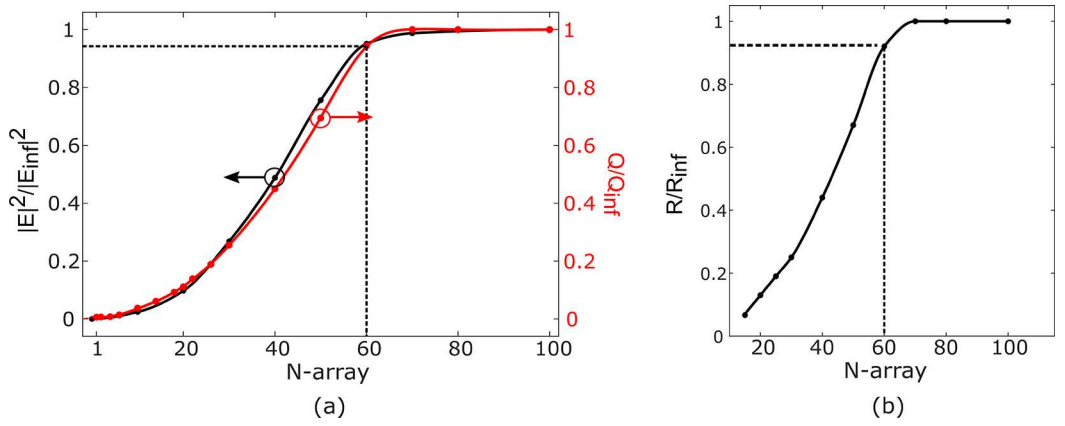

Figure 3. (a) Energy values (black curve) and *Q*-factor (red curve) and (b) reflectance normalized to the values obtained with an infinite array as a function of the array elements N. The dotted lines indicate the performance obtained with $N = 60$.

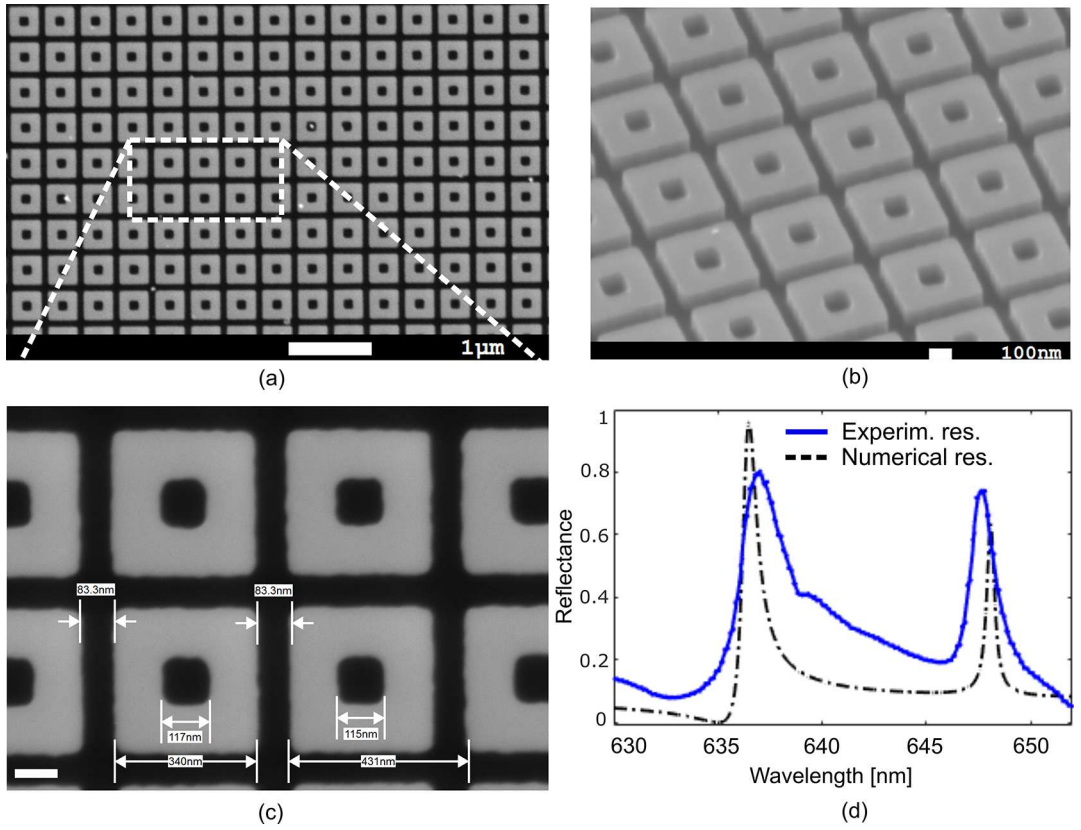

Figure 4. (a–c) SEM micrographs of the nanocuboid array at different magnifications (see scale bar) and (d) comparison of the experimental reflection spectrum (blue curve) with the numerical calculation (black curve).

the desired strong energy localization and is therefore not considered here.

We select a thickness $t = 100$ nm for the amorphous silicon thin film and a side length $b = 120$ nm for the inscribed square, which we define as the nanocuboid core, both for reasons of fabrication limitations and because our target objects are viruses of typically 100 nm size. Regarding the gap g that separates the cuboids, we note that the simulation in ref 28 uses an aspect ratio between t and g of almost 10:1 in order to achieve the reported high *Q*-factors, yet such narrow gaps which would be extremely difficult to fabricate with high quality; instead, we chose a ratio nearer 1:1, that is, a gap size of $g = 90$ nm to ensure reliable fabrication. Our numerical simulations (Supporting Information, S1) indicate a *Q*-factor of $Q = 800$ with a strong resonance amplitude ($R \sim 1$) for this design. We also note that other configurations may provide higher *Q*-values, but these may also reduce the confinement energy inside the cuboid on resonance (Supporting Information, S1), which would reduce the trapping force. In fact, a *Q*-factor around $Q \sim 1000$ is advantageous for the envisaged trapping application, as the resonance detunes when the particle enters the trapping site; for higher *Q*-factors, the change in resonance wavelength upon trapping would be larger than the line width of the resonance and detune the trap off-resonance altogether.[30] Therefore, the metasurface should

https://doi.org/10.1021/acsphotonics.1c00354
ACS Photonics 2021, 8, 2060–2066

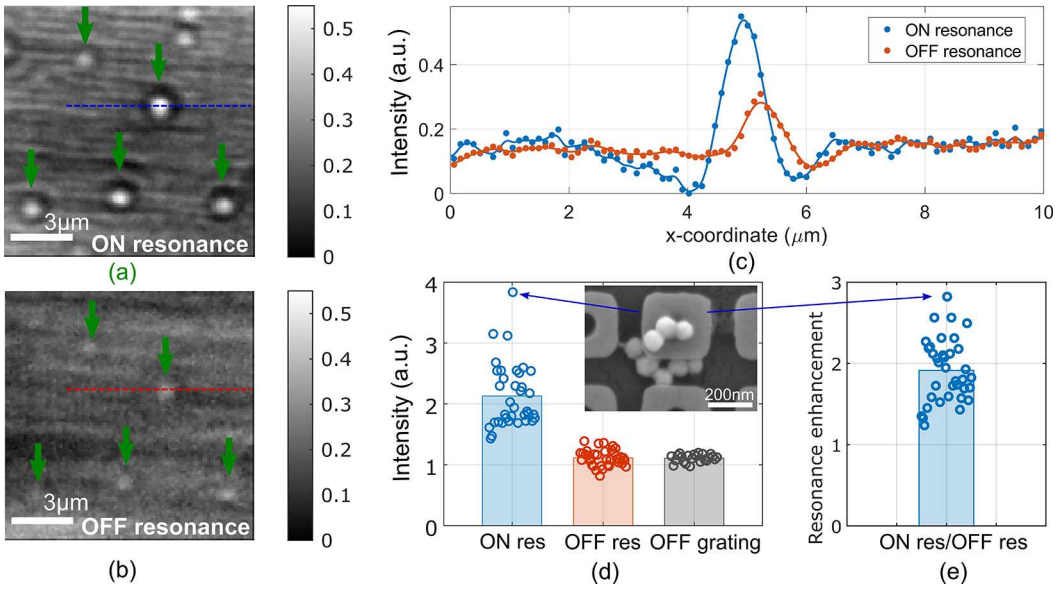

Figure 5. Microscope images of 80 nm Au bead deposited on the dielectric metasurface in (a) on-resonance and (b) off-resonance condition. (c) Comparison of the intensity profile of the scattering signal from the same Au bead in on-resonance (blue curve) and off-resonance (red curve) condition. (d) Histogram of the average intensity of the scattering signal from 33 particles (dots) at resonance (blue), off-resonance (red) and off-grating (black), normalized to the background signal. (e) Intensity ratio of the scattering signal from the same particles between on-resonance and off-resonance condition.

provide a resonance line width comparable to or larger than the spectral shift observed upon trapping.

The reflection spectrum shown in Figure 2 assumes an infinite array of nanocuboids (similar to ref 28), but we note that the resonance is affected by the size of the array; starting from an infinite array, we observe a decrease of the resonance amplitude and Q-factor once the array drops below $N = 60$ (Figure 3).

Array size also matters in terms of total power; clearly, if the best performance was only achieved for an infinite array, then the illumination power would also have to be infinite, which is clearly impractical. In Optical Trapping Considerations, we consider the optical power requirement for trapping in order to understand whether it is realistic to operate with such a large number of trapping sites.

Fabrication and Experimental Results. We fabricated the metasurface in oxygen-rich hydrogenated amorphous silicon (a-SiOx:H) and used e-beam lithography and reactive-ion etching to define the nanostructure;[28] SEM micrographs are shown in Figure 4a–c. The reflection spectrum is shown in Figure 4d and was obtained with a normally incident collimated beam from an unpolarised halogen source filtered through a monochromator; all spectra are normalized to a silver mirror. We observe a Q-factor ~350 and a peak reflectivity $R = 0.8$. The reduction of the Q-factor compared to the numerical result ($Q_{sim} = 800$, Figure 4b) can be explained by fabrication imperfections, but as we discuss below, this value is already sufficient for the intended multiple trapping application.

We have experimentally verified the strong near-field confinement of the dielectric metasurface, by comparing the scattering signal collected by 80 nm Au beads deposited on the metasurface in on-resonance and off-resonance condition. For these measurements, an optical setup working with transmitted light has been used, obtaining a dip in transmission when the input wavelength matches the resonance condition of the metasurface array. A 60× objective with NA = 0.95 is used to collect the transmitted signal, which is then sent to a CMOS camera in order to detect the scattering from one or a few scatterers. We have applied 80 nm Au beads, initially suspended in water, and allowed them to settle on the metasurface by letting the water evaporate. We then tuned the wavelength from "on-resonance to "off-resonance" in order to see the difference in scattering from those particles that accidentally landed on a hotspot. As shown in Figure 5a,b, the scattering signal collected at resonance from the Au beads is remarkably higher by a factor of 2–3 than the intensity observed from the same beads in off-resonance condition (Figure 5c). Both images were taken with the same camera settings and plotted with the same intensity range for a direct comparison. The scattering contribution is almost negligible off-resonance and off-grating (Figure 5d,e), which clearly confirms that the resonance enhancement is playing a significant role.

Optical Trapping Considerations. We conducted 3D FEM simulations and applied the Maxwell Stress Tensor (MST) method to calculate the optical forces exerted by the array on a 100 nm particle with a refractive index $n = 1.45$, representing the properties of a virus,[21] immersed in water ($n = 1.33$). The method used to calculate the optical forces is described in ref 31. The results are shown in Figure 6, which are based on the experimental values shown in Figure 4d and Supporting Information, S3. We use the optical stability as an indicator for trapping efficiency; the stability is defined as $S = U/(k_B \cdot T_c)$, where U is the potential energy that corresponds to the work required to bring the nanoparticle from a free position to the trapping site, k_B is the Boltzmann constant, and T_c is the temperature in Kelvin.[15] A stability of $S \geq 1$ is required to ensure that the trapping force acting on the object is stronger than the opposite force exerted by thermal effects. Higher stability corresponds to longer trapping time; for example, a trapping time of several seconds has been observed with other dielectric nanotweezers of $S \sim 1$.[14] For this condition, dynamic trapping in the array is guaranteed, due to

https://doi.org/10.1021/acsphotonics.1c00354
ACS Photonics 2021, 8, 2060–2066

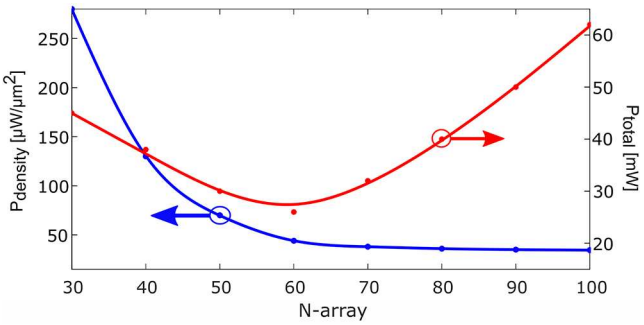

Figure 6. Power density in each single cell (blue curve) and total power (red curve) as a function of the array size N.

the fact that the trapping event is long enough to allow the characterization of each single particle[32] before it is released from the trap and replaced with different particles in solution. We, therefore, suggest that $S \sim 1$ is a good target value for studying the heterogeneity of a larger population of bioparticles.

Figure 6 shows that the power density, defined as the power per trapping site to reach a stability of $S = 1$, drops with increasing array size and reaches a value of around 39 $\mu W/\mu m^2$ for an array size of $N \geq 60$, while the total power is minimal for $N = 60$. The minimum power obtained for $N = 60$ is due to the combination of resonant field enhancement and strong amplitude of resonance, both of which enhance the optical forces and allow us to reach the stability criterion $S = 1$ with lower power density. We note that the total power for $N = 60$ is $P \approx 26$ mW, which is a value that can be readily achieved with a tunable laser, thereby indicating that it is realistic to achieve trapping of thousands of objects in parallel with the structure discussed here. Given that the metasurface is realized in a low-loss dielectric system, we can also expect for heating effects to be minimal, confirming the suitability of the system for trapping biological objects, both in terms of avoiding thermal convection currents and avoiding thermal damage.

Finally, we consider the trapping site, since it is desirable to localize the particle in a defined position within the array. For example, the particle might be trapped by the hotspot in the gap separating adjacent nanocuboids. As shown in Figure 7, this is not the case, and the simulation clearly shows a ≈2× stronger force exerted by the central core than by the gap (Figure 7b). Nevertheless, the gradient field associated with the gap provides an auxiliary effect, because it helps to draw particles closer to the sensor surface and guiding them to the trapping site.

Assuming the experiment is conducted with a single wavelength source at $\lambda = 636$ nm, matching with the resonance condition of the metasurface when the traps are filled, a resonance shift of $\Delta\lambda = 1.05$ nm is obtained in the presence of

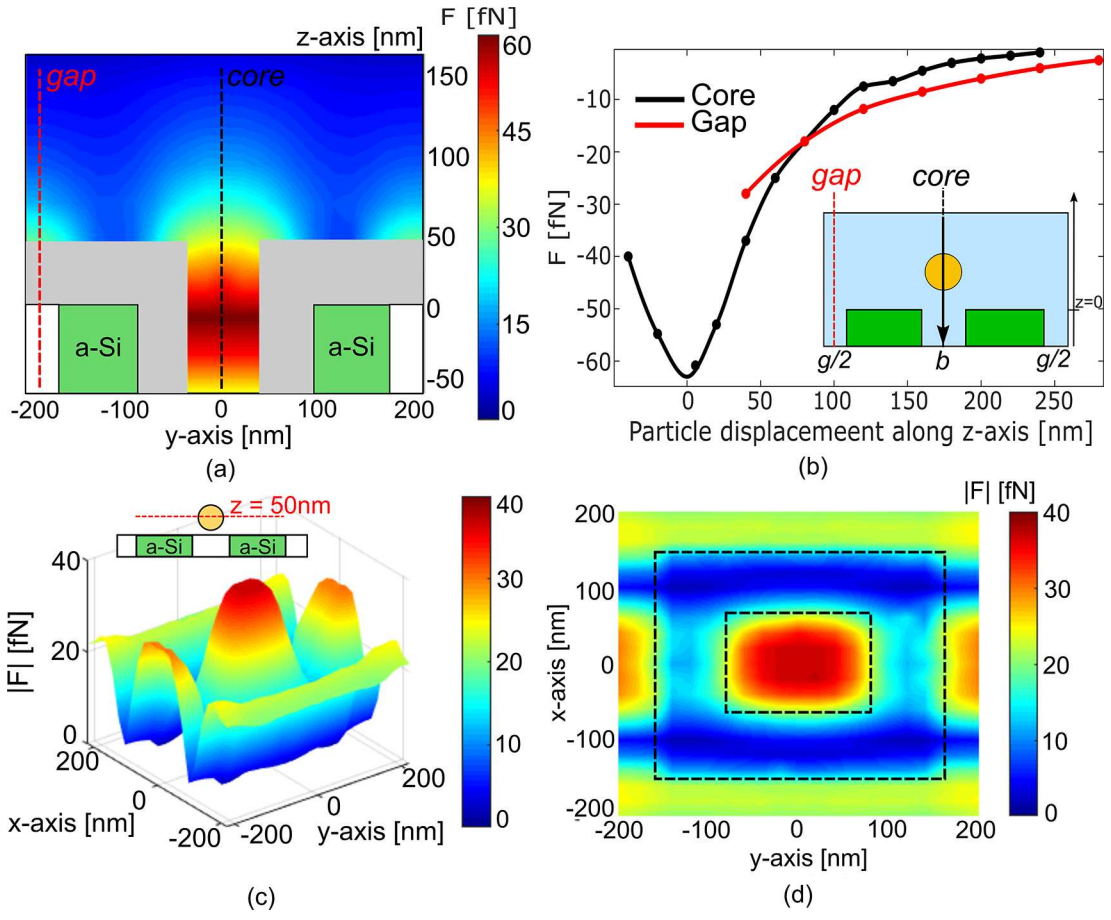

Figure 7. (a) Optical forces exerted on a 100 nm bead in the cross-section of the unit cell. Assuming each point as the position of the center of the bead, the gray area represents the positions not allowed for the bead. (b) Comparison of forces obtained by displacing the bead along the z-axis above the hollow core (black curve) and the gap (red curve) with a schematic of the geometry in the inset. (c) Force distribution and (d) top view of the optical forces in the plane $z = 50$ nm above the surface of the device. The dotted lines indicate the geometry of the unit cell.

https://doi.org/10.1021/acsphotonics.1c00354
ACS Photonics 2021, 8, 2060−2066

a trapping event, with a corresponding change in reflectance of $\Delta R = 0.55$. This shift in resonance and transmission is given by the coupling between the particle and the optical field in the trap, generating a self-induced back-action (SIBA) effect,[33] for which the particle itself contributes actively to the trapping action. Once trapped, any movement of the particle away from the trapping site translates into a restoring force toward the trap because the system aims to maintain its lowest energy state.[30]

Furthermore, we have investigated the impact of adjacent optical traps on a specific trapping site, which is important to study multiple trapping (see Supporting Information, S3 for more details).

We have also verified the operation of the metasurface for the trapping of biological objects in the size range 80−120 nm, in order to confirm the suitability of the structure for the trapping of the most common viruses such as influenza and coronavirus[34,35] (see Supporting Information, S4).

Having extracted quantitative results from the simulation, we can now compare our dielectric metasurface to other array trapping modalities and assess how the total power of ≈26 mW required for thousands of trapping sites compares. For example, the nanojet array described in ref 10 has achieved the parallel trapping of a maximum of 60 objects with a total power of 60 mW. The plasmonic array reported in ref 36 has demonstrated the parallel trapping of five objects with a total power of about 20 mW, although it could be scaled up further, because of the availability of a larger number of nanotraps; both of these modalities require a power higher than hundreds of microwatts per trapping site, while the structure presented here operates at 7 μW/site. From this comparison it is clear that the dielectric metasurface approach offers significant advantages and that an experimental demonstration has considerable promise. Regarding this future experimental demonstration, it would also be useful to better understand the impact of the design on the array size. It is clear, for example, that the gap g controls the coupling between adjacent nanocuboids; for a very narrow gap, as in ref 28, the cuboids are coupled more strongly, which is responsible for the high Q-factor, but also requires a larger array; in contrast, if g was chosen larger than the value of $g = 95$ nm used here, we can expect the Q-factor and the energy confinement to drop, but the array could be made smaller.

In addition to the possibility of studying the heterogeneity of large populations, we can also foresee the use of the array toward fluorescence or Raman spectroscopy studies.[37,38] The ability to localize multiple individual particles in a small volume, thereby minimizing their movement, strongly minimizes the background noise compared to unconstrained objects in bulk solutions thereby improving the signal-to-noise ratio of the measurement.

CONCLUSIONS

We have considered the requirements for a nanostructure that enables the multiplexed near-field optical trapping of a large number of biological objects such as viruses. Having considered the various options, including nanojets and plasmonic arrays, we believe that an approach based on a dielectric metasurface has considerable promise. The structure we put forward supports an anapole mode that provides strong near-field confinement together with a relatively high Q-factor and resonance amplitude. We have designed and fabricated the metasurface and show a good agreement between its simulated and experimental properties, in particular, an experimental Q-factor of ∼350 and a peak reflectivity $R = 0.8$, which indicates strong energy localization in the resonance. Our numerical results, based on these results, confirm that thousands of 100 nm particles such as viruses could be trapped in a 60 × 60 array simultaneously with a total input power $P \sim 26$ mW or 7 μW/trapping site. This possibility of optically trapping a large number of objects in parallel with a limited power and without complex setups will open up new studies in many fields of biology and medicine, such as in microbiology, virology, and immunology, for the study of pathogens such as viruses in combination with Raman spectroscopy or fluorescence.

ASSOCIATED CONTENT

Supporting Information

The Supporting Information is available free of charge at https://pubs.acs.org/doi/10.1021/acsphotonics.1c00354.

Design of the metasurface, comparison of performance for different array size, impact of adjacent traps on a single site for dynamic multiple trapping, and optical forces for different particles size (PDF)

AUTHOR INFORMATION

Corresponding Author

Caterina Ciminelli − *Optoelectronics Laboratory, Politecnico di Bari, 70125 Bari, Italy;* orcid.org/0000-0001-8724-016X; Email: caterina.ciminelli@poliba.it

Authors

Donato Conteduca − *Photonics Group, Department of Physics, University of York, York YO10 5DD, United Kingdom*

Giuseppe Brunetti − *Optoelectronics Laboratory, Politecnico di Bari, 70125 Bari, Italy*

Giampaolo Pitruzzello − *Photonics Group, Department of Physics, University of York, York YO10 5DD, United Kingdom*

Francesco Tragni − *Optoelectronics Laboratory, Politecnico di Bari, 70125 Bari, Italy*

Kishan Dholakia − *SUPA, School of Physics and Astronomy, University of St Andrews, St Andrews KY16 9SS, United Kingdom*

Thomas F. Krauss − *Photonics Group, Department of Physics, University of York, York YO10 5DD, United Kingdom;* orcid.org/0000-0003-4367-6601

Complete contact information is available at: https://pubs.acs.org/10.1021/acsphotonics.1c00354

Funding

The authors G. B., F. T., and C. C acknowledge financial support by the POR of Apulia region, IT (FESR FSR 2014−2020, Action 10.4, "Research for Innovation" (REFIN) Initiative). The authors D.C., G.P., K.D., and T.F.K. acknowledge financial support by the EPSRC of the UK (Grant EP/P030017/1).

Notes

The authors declare no competing financial interest.

REFERENCES

(1) Ashok, P. C.; Dholakia, K. Optical trapping for analytical biotechnology. *Curr. Opin. Biotechnol.* **2012**, *23* (1), 16−21.

(2) Ashkin, A.; Dziedzic, J. M.; Yamane, T. Optical trapping and manipulation of single cells using infrared laser beams. *Nature* **1987**, *330*, 769−771.
(3) Marago, O. M.; Jones, P. H.; Gucciardi, P. G.; Volpe, G.; Ferrari, A. Optical trapping and manipulation of nanostructures. *Nat. Nanotechnol.* **2013**, *8* (11), 807−819.
(4) Pang, Y.; Gordon, R. Optical Trapping of a Single Protein. *Nano Lett.* **2012**, *12* (1), 402−406.
(5) Kotnala, A.; Gordon, R. Double nanohole optical tweezers visualize protein p53 suppressing unzipping of single DNA-hairpins. *Biomed. Opt. Express* **2014**, *5* (6), 1886−1894.
(6) Yoo, D.; Gurunatha, K. L.; Choi, H.-K.; Mohr, D. A.; Ertsgaard, C. T.; Gordon, R.; Oh, S.-H. Low-Power Optical Trapping of Nanoparticles and Proteins with Resonant Coaxial Nanoaperture Using 10 nm Gap. *Nano Lett.* **2018**, *18* (6), 3637−3642.
(7) Lidstrom, M. E.; Konopka, M. C. The role of physiological heterogeneity in microbial population behavior. *Nat. Chem. Biol.* **2010**, *6*, 705−712.
(8) Armbrecht, L.; Dittrich, P. S. Recent Advances in the Analysis of Single Cells. *Anal. Chem.* **2017**, *89* (1), 2−21.
(9) Ozcelik, D.; Jain, A.; Stambaugh, A.; Stott, M. A.; Parks, J. W.; Hawkins, A.; Schmidt, H. Scalable Spatial-Spectral Multiplexing of Single-Virus Detection Using Multimode Interference Waveguides. *Sci. Rep.* **2017**, *7*, 12199.
(10) Li, Y.; Xin, H.; Liu, X.; Zhang, Y.; Lei, H.; Li, B. Trapping and detection of nanoparticles and cells using a parallel photonic nanojet array. *ACS Nano* **2016**, *10* (6), 5800−5808.
(11) Daly, M.; Sergides, M.; Nic Chormaic, S. Optical trapping and manipulation of micrometer and submicrometer particles. *Laser Phot. Rev.* **2015**, *9*, 309−329.
(12) Ghosh, S.; Ghosh, A. Next-generation optical nanotweezersfor dynamic manipulation:from surface to bulk. *Langmuir* **2020**, *36*, 5691−5708.
(13) Conteduca, D.; Dell'Olio, F.; Krauss, T. F.; Ciminelli, C. Photonic and plasmonic nanotweezing of nano- and microscale particles. *Appl. Spectrosc.* **2017**, *71* (3), 367−390.
(14) Xu, Z.; Song, W.; Crozier, K. B. Optical trapping of nanoparticles using all-silicon nanoantennas. *ACS Photonics* **2018**, *5* (12), 4993−5001.
(15) Conteduca, D.; Reardon, C. P.; Scullion, M.; Dell'Olio, F.; Armenise, M. N.; Krauss, T. F.; Ciminelli, C. Ultra-high Q/V hybrid cavity for strong light matter interaction. *APL Photonics* **2017**, *2*, 086101.
(16) Kotsifaki, D. G.; Truong, V. G.; Chormaic, S. N. Fano-Resonant, Asymmetric, Metamaterial-Assisted Tweezers for Single Nanoparticle Trapping. *Nano Lett.* **2020**, *20*, 3388−3395.
(17) Han, X.; Truong, V. G.; Thomas, P. S.; Nic Chormaic, S. Sequential trapping of single nanoparticles using a gold plasmonic nanohole array. *Photonics Res.* **2018**, *6* (10), 981−985.
(18) Han, S.; Shi, Y. Systematic analysis of optical gradient force in photonic crystal nanobeam cavities. *Opt. Express* **2016**, *24* (1), 452−458.
(19) Conteduca, D.; Dell'Olio, F.; Ciminelli, C.; Krauss, T. F.; Armenise, M. N. Design of a high performance optical tweezer for nanoparticle trapping. *Appl. Phys. A: Mater. Sci. Process.* **2016**, *122* (4), 295.
(20) Erickson, D.; Serey, X.; Chen, Y.-F.; Mandal, S. Nano-manipulation using near field photonics. *Lab Chip* **2011**, *11*, 995−1009.
(21) Pang, Y.; Song, H.; Cheng, W. Using optical trap to measure the refractive index of a single animal virus in culture fluid with high precision. *Biomed. Opt. Express* **2016**, *7* (5), 1672−1689.
(22) Jones, J.E.; Le Sage, V.; Lakdawala, S.S. Viral and host heterogeneity and their effects on the viral life cycle. *Nat. Rev. Microbiol.* **2021**, *19*, 272−282.
(23) Tadesse, L. F.; Safir, F.; Ho, C.-S.; Hasbach, X.; Yakub, B. K.; Jeffrey, S. S.; Saleh, A. A. E.; Dionne, J. Toward rapid infectious disease diagnosis with advances in surface-enhance Raman spectroscopy. *J. Chem. Phys.* **2020**, *152*, 240902.
(24) Weaver, W. M.; Tseng, P.; Kunze, A.; Masaeli, M.; Chung, A.; Dudani, J. S.; Kittur, H.; Kulkarni, R. P.; Di Carlo, D. Advances in high-throughput single-cells microtechnologies. *Curr. Opin. Biotechnol.* **2014**, *25*, 114−123.
(25) Svahn, H. A.; Van der Berg, A. Single cells or large populations? *Lab Chip* **2007**, *7* (5), 544−546.
(26) Conteduca, D.; Barth, I.; Pitruzzello, G.; Reardon, C. P.; Martins, E. R.; Krauss, T. F. Dielectric nanohole array metasurface for high-resolution near-field sensing and imaging. *Nat. Commun.* **2021**, *12*, 3293.
(27) Neuman, K. C.; Block, S. M. Optical Trapping. *Rev. Sci. Instrum.* **2004**, *75* (9), 2787−2809.
(28) Algorri, J. F.; Zografopoulos, D. C.; Ferraro, A.; Garcia-Camara, B.; Beccherelli, R.; Sanchez-Pena, J. M. Ultrahigh quality factor resonant dielectric metasurfaces based on hollow nanocuboids. *Opt. Express* **2019**, *27* (5), 6320−6330.
(29) Koshelev, K.; Favraud, G.; Bogdanov, A.; Kivshar, Y.; Fratalocchi, A. Nonradiating photonics with resonant dielectric nanostructures. *Nanophotonics* **2019**, *8* (5), 725.
(30) Descharmes, N.; Dharanipathy, U. P.; Diao, Z.; Tonin, M.; Houdre, R. Observation of backaction and self-induced trapping in a planar hollow photonic crystal cavity. *Phys. Rev. Lett.* **2013**, *110* (12), 123601.
(31) Ciminelli, C.; Conteduca, D.; Dell'Olio, F.; Armenise, M.N. Design of an optical trapping device based on an ultra-high Q/V resonant structure. *IEEE Phot. Journal* **2014**, *6* (6), 0600916.
(32) Yuan, Y.; Lin, Y.; Gu, B.; Panwar, N.; Tjin, S. C.; Song, J.; Qu, J.; Yong, K.-T. Optical trapping-assisted SERS platforms for chemical and biosensing applications: Design perspectives. *Coord. Chem. Rev.* **2017**, *339*, 138−152.
(33) Juan, M. L.; Gordon, R.; Pang, Y.; Eftekhari, F.; Quidant, R. Self-induced back-action optical trapping of dielectric nanoparticles. *Nat. Phys.* **2009**, *5*, 915−919.
(34) Guy, J. S.; Breslin, J. J.; Breuhaus, B.; Vivrette, S.; Smith, L. G. Characterization of a coronavirus isolated from a diarrheic foal. *J. Clin. Microbiol.* **2000**, *38* (12), 4523−4526.
(35) Vajda, J.; Weber, D.; Brekel, D.; Hundt, B.; Muller, E. Size distribution analysis of influenza virus particles using size exclusion chromatography. *J. of Chrom.* **2016**, *1465*, 117−125.
(36) Kotsifaki, D. G.; Truong, V. G.; Nic Chormaic, S. Dynamic multiple nanoparticle trapping using metamaterial plasmonic tweezers. *Appl. Phys. Lett.* **2021**, *118*, 021107.
(37) Huang, J.; Mousavi, M. Z.; Zhao, Y.; Hubarevich, A.; Omeis, F.; Giovannini, G.; Schutte, M.; Garoli, D.; De Angelis, F. SERS discrimination of single DNA bases in single oligonucleotides by electro-plasmonic trapping. *Nature Comm.* **2019**, *10*, 5321.
(38) Jones, S.; Al Balushi, A. A.; Gordon, R. Raman spectroscopy of single nanoparticles in a double-nanohole optical tweezer system. *J. Opt.* **2015**, *17*, 102001.

https://doi.org/10.1021/acsphotonics.1c00354
ACS Photonics 2021, 8, 2060−2066